JOURNAL OF GUIDANCE, CONTROL, AND DYNAMICS
Vol. 35, No. 4, July–August 2012

Covariance-Based Realization Algorithm for the Identification of Aeroelastic Dynamics

Daniel N. Miller* and Raymond A. de Callafon†
University of California, San Diego, La Jolla, California 92093-0411
and
Martin J. Brenner‡
NASA Dryden Flight Research Center, Edwards, California 93523-0273

DOI: 10.2514/1.55770

A novel subspace system identification method based on covariance estimates and inspired by classical realization techniques is presented that constructs system estimates from measured input–output data. The resulting algorithm allows for the identification of parametric system models from data sets of large signal dimension and is applicable to data perturbed by colored noise and acquired in closed-loop operation due to the unbiased estimation of cross-covariance functions, even in low signal-to-noise conditions. The algorithm is applied to data measured onboard an F/A-18. The results demonstrate the effectiveness of the algorithm in efficiently computing accurate, unbiased linear dynamic models from large data sets of high-dimensional signal sets obtained from aircraft in flight.

I. Introduction

VIBRATIONS due to aeroservoelastic (ASE) dynamics of aircraft structures, commonly referred to as flutter, have the potential to damage and destroy aircraft in flight if not properly analyzed and suppressed. The current trend in the analysis of ASE dynamics is to derive finite element and computational-fluid-dynamic models of an airframe at various flight conditions, and to interpolate and extrapolate the damping of flutter modes across the full flight envelope. These computational models are then validated through ground testing and, finally, in-flight testing before the aircraft can be considered operationally safe [1].

In-flight analysis of flutter, however, is inherently difficult due not only to its dangerous nature but also to the unsteady, turbulent phenomena that induce it. These effects manifest themselves as essentially nondeterministic disturbances, or noise, on acquired data. By nature, this noise is colored and correlated across all measured signals; perturbations on control-surface positions due to turbulent airflow are inherently correlated with the perturbations measured in stress and acceleration on the aircraft. Attempts to analyze data generated from in-flight experiments must take these facts into account to avoid inaccurate conclusions.

Most system identification methods assume that the noise on measured signals is either white, uncorrelated, or both, and are thus ill-suited for identifying ASE dynamics. When dealing with experimental data that do not meet these assumptions, techniques from the analysis of stochastic processes must be incorporated into the identification methods used. Additionally, many system-identification methods are based on nonlinear optimizations over cost functions that become extremely nonconvex for large high-dimensional data sets, making them infeasible for ASE analysis, in which many sensors are employed to capture the behavior of the airframe.

Traditional subspace methods [2] have been previously applied to the identification of aeroelastic dynamics using simulated data from an F-16 aircraft and measured data from a V-22 rotorcraft [3]. Such methods assume strictly deterministic inputs in order to remove the effects of subsequent input on the propagation of the state dynamics and in order to decorrelate the deterministic and nondeterministic subsystems. A subspace-based method for online monitoring of aeroelastic damping was developed and applied to in-flight data by Mevel et al [4]. This method used output data only and relied on the autocovariance of the data to determine when statistically significant damping of vibration modes dropped below a given threshold but did not identify the input–output behavior of the aeroelastic phenomena and assumed no deterministic control-surface excitation during data acquisition. This method was later extended to include known, strictly deterministic inputs [5].

These previous studies all assume disturbances to be white, which in practice is often insufficient. Nondeterministic effects from turbulence, sensor noise, and, in the closed-loop case, control-system feedback will inevitably produce colored noise on the output data. In such cases, either the modes of the estimated system will be biased by the disturbance spectrum ([6], pages 253–254), or, if the model order is chosen to be artificially high, the observable modes of the strictly nondeterministic subsystem will be estimated alongside the modes of the deterministic subsystem but be incorrectly identified as controllable [7]. This is particularly problematic if the dynamic model is intended to be used for active flutter suppression, as the control algorithm designed from the derived model will attempt to control the uncontrollable modes. Additionally, treatment of the input as strictly deterministic is only possible if the input measured is actuator commands. In this case, the derived model will include actuator dynamics (such as servomotor dynamics) as well as aeroelastic dynamics. If actuator positions are measured instead, the position measurements will include perturbations that are correlated with the noise on the measured output data, and the effects of the input on state dynamics cannot be removed with the standard methods of orthogonal projections.

Alternative proposed methods of estimating ASE dynamics include applying frequency-domain total least squares by restricting the identification to error-in-variables models [8], which allows for the incorporation of colored noise. An approach based on rational orthogonal basis functions incorporated static input and output nonlinearities and addressed the issue of identifying parameter-varying models [9]. Neither allows for the presence of correlated noise on both the input and output measurements and, unlike subspace methods, these methods all require a priori parameterization of the dynamic system.

Received 26 July 2011; revision received 8 February 2012; accepted for publication 30 January 2012.

*Graduate Student, Department of Mechanical and Aerospace Engineering; d6miller@ucsd.edu. Student Member AIAA.
†Professor, Department of Mechanical and Aerospace Engineering; callafon@ucsd.edu.
‡Aerospace Engineer, martin.j.brenner@nasa.gov. Senior Member AIAA.

Subspace identification refers to a broad class of system identification methods that estimate system dynamics without the need for iterative or nonlinear numerical tools. The general approach of such methods is to estimate state-space system parameters from the row space of some alternative matrix constructed from measured data. Although some notable exceptions exist, by far the most common approach, and the one used in this paper, is to construct block-Hankel matrices of measured data, and then use various projection operations to isolate the free response of the system at subsequent time steps [2].

The goal of this paper is to present a system identification method that addresses these difficulties and is appropriate for the identification of aeroelastically induced vibration modes. The method computes a linear dynamic system in the presence of colored and correlated noise on both input and output measurements while remaining scalable to large high-dimensional data sets. The method uses estimated cross-covariance functions between signals to reduce the effects of noise and focus on only the input–output behavior of a system. The result is a subspace identification algorithm that generalizes realization theory by incorporating results from stochastic processes and is thereby referred to as a covariance-based realization algorithm (COBRA) by the authors. The algorithm possesses resemblance to and inspiration from the eigensystem realization algorithm (ERA) [10] and the commonly associated observer/Kalman filter identification (OKID) [11], methods frequently used in the aerospace community.

Existing subspace methods implicitly assume that covariance functions are calculated when structured matrices of data are multiplied together to isolate the system dynamics, including newly developed "predictor-based" methods [12]. These methods assume that certain matrix products approach matrices of covariance functions as the dimensions of the data matrices become infinite. This approach can be problematic for data sets in which the input or output signals are of high dimension, as the sizes of the data matrices grow so quickly that the matrix products become infeasible to compute. In contrast, our method computes covariance-function estimates beforehand so that the size of the data matrices remains fixed, allowing for the use of much larger data sets than with other subspace methods.

The following section of the paper describes the algorithm in detail. The algorithm is then applied to data measured from in-flight experiments with a discussion of the various sources of bias that would result were the identification to be performed from the input–output data alone. It is shown that COBRA is effective in modeling induced vibration modes for in-flight experiments. Results and future work are discussed in the Conclusions (Sec. IV), and the relationship of the algorithm to similar known methods is discussed in the Appendix.

II. Identification from Dynamic Invariance

This section describes the algorithm to be later applied to the identification of ASE dynamics. After providing a preliminary background on stochastic processes necessary to define notation and assumptions on the measured signals, we demonstrate how shifted data matrices can be used to estimate the discrete-time invariant dynamics responsible for propagating the state over samples of measured data.

A. Preliminary Theory of Stochastic Processes

In the following, the time t is assumed to be an integer index rather than a continuous time variable. A signal $s(t) \in \mathbb{R}^{n_s}$ is said to be quasi stationary if it satisfies the two conditions

$$Es(t) = m_s(t), \qquad \|m_s(t)\|_2 \leq C \tag{1}$$

and

$$R_s(\tau) = \lim_{N\to\infty} \frac{1}{N} \sum_{t=0}^{N} Es(t+\tau)s(t)^T, \qquad \|R_s(\tau)\|_2 \leq C \tag{2}$$

for some $C < \infty$, where E denotes expectation, which has no effect if $s(t)$ is strictly deterministic. The function $R_s(\tau)$ is called the autocovariance function of $s(t)$. Similarly, if $w(t) \in \mathbb{R}^{n_w}$ is a second quasi-stationary signal, then the function

$$R_{sw}(\tau) = \lim_{N\to\infty} \frac{1}{N} \sum_{t=0}^{N} Es(t+\tau)w(t)^T$$

is called the cross-covariance function of $s(t)$ and $w(t)$. If only N samples of data are available, the autocovariance and cross-covariance-function estimates

$$\hat{R}_s(\tau) = \frac{1}{N} \sum_{t=0}^{N} s(t+\tau)s(t)^T \qquad \hat{R}_{sw}(\tau) = \frac{1}{N} \sum_{t=0}^{N} s(t+\tau)w(t)^T \tag{3}$$

converge to $R_s(\tau)$ and $R_{sw}(\tau)$, respectively, as $N \to \infty$ ([13], page 32). If $S(e^{j\omega})$ and $W(e^{j\omega})$ are the Fourier transforms of signals $s(t)$ and $w(t)$, respectively, then their cross-covariance-function estimate may be computed as

$$\hat{R}_{sw}(\tau) = \mathcal{F}^{-1}[S(e^{j\omega})W(e^{j\omega})^*]$$

where $\mathcal{F}^{-1}$ indicates the inverse Fourier transform and $(\cdot)^*$ represents the complex-conjugate transpose. In this paper, all signals are restricted to being quasi stationary and zero mean.

Next, consider a linear time-invariant discrete-time system described by the state-space equations

$$x(t+1) = Ax(t) + Bu(t) \qquad y(t) = Cx(t) + Du(t) + v(t) \tag{4}$$

which relate the input $u(t) \in \mathbb{R}^{n_u}$ to the state $x(t) \in \mathbb{R}^n$ and the output $y(t) \in \mathbb{R}^{n_y}$ in terms of the constant matrices $A \in \mathbb{R}^{n\times n}$, $B \in \mathbb{R}^{n\times n_u}$, $C \in \mathbb{R}^{n_y\times n}$, and $D \in \mathbb{R}^{n_y\times n_u}$. Added to the output is a possibly colored noise signal $v(t) \in \mathbb{R}^{n_y}$, assumed to be the realization of a stationary, stochastic process that may or may not share dynamics with the system described by (A, B, C, D). We limit Eq. (4) to include only minimal realizations [14] of stable systems.

If $\xi(t) \in \mathbb{R}^{n_\xi}$ is a signal that is correlated with $u(t)$ and $v(t)$, then the cross-covariance functions $R_{u\xi}(\tau) \in \mathbb{R}^{n_u\times n_\xi}$, $R_{y\xi}(\tau) \in \mathbb{R}^{n_y\times n_\xi}$, and $R_{v\xi}(\tau) \in \mathbb{R}^{n_y\times n_\xi}$ will exist. If we define the cross covariance of the state with $\xi(t)$ as $R_{x\xi}(\tau) \in \mathbb{R}^{n\times n_\xi}$, then the covariance functions may be expressed in terms of the state-space matrices (A, B, C, D) as

$$\begin{aligned} R_{x\xi}(\tau+1) &= AR_{x\xi}(\tau) + BR_{u\xi}(\tau) \\ R_{y\xi}(\tau) &= CR_{x\xi}(\tau) + DR_{u\xi}(\tau) + R_{v\xi}(\tau) \end{aligned} \tag{5}$$

If, however, $\xi(t)$ is chosen such that it is correlated with $u(t)$ but uncorrelated with $v(t)$, then

$$R_{v\xi}(\tau) = 0 \quad \forall\ \tau \tag{6}$$

and the relationship between $R_{u\xi}(\tau)$ and $R_{y\xi}(\tau)$ will be limited to the dynamics of the deterministic subsystem. Examples of such $\xi(t)$ include $u(t)$ if it is unperturbed by noise correlated with $v(t)$ and the system is in open-loop operation, or an external reference signal if the data is measured in closed-loop operation ([13], page 434).

B. Identification from Dynamic Invariance of Covariance Functions

Let $\hat{R}_{y\xi}(\tau)$ be an estimate of the cross-covariance function $R_{y\xi}(\tau)$, as defined in Eq. (3), computed over some domain $\tau \in [\tau_{\min}, \tau_{\max}]$. A block-Hankel matrix consisting of l block columns of i length sequences of $\hat{R}_{y\xi}(\tau)$

$$\mathbf{R}_{y\xi} = \begin{bmatrix} \hat{R}_{y\xi}(\tau_{\min}) & \hat{R}_{y\xi}(\tau_{\min}+1) & \cdots & \hat{R}_{y\xi}(\tau_{\min}+l-1) \\ \hat{R}_{y\xi}(\tau_{\min}+1) & \hat{R}_{y\xi}(\tau_{\min}+2) & \cdots & \hat{R}_{y\xi}(\tau_{\min}+l) \\ \vdots & \vdots & & \vdots \\ \hat{R}_{y\xi}(\tau_{\min}+i-1) & \hat{R}_{y\xi}(\tau_{\min}+i) & \cdots & \hat{R}_{y\xi}(\tau_{\min}+i+l-2) \end{bmatrix} \in \mathbb{R}^{in_y \times ln_\xi}$$

may be expressed as

$$\mathbf{R}_{y\xi} = \Gamma \mathbf{R}_{x\xi} + T\mathbf{R}_{u\xi} + \mathbf{R}_{v\xi} \tag{7}$$

in which

$$\Gamma = [\, C^T \quad (CA)^T \quad (CA^2)^T \quad \cdots \quad (CA^{i-1})^T \,]^T \in \mathbb{R}^{in_y \times n} \tag{8}$$

is the extended observability matrix,

$$\mathbf{R}_{x\xi} = [\, \hat{R}_{x\xi}(\tau_{\min}) \quad \hat{R}_{x\xi}(\tau_{\min}+1) \quad \cdots \quad \hat{R}_{x\xi}(\tau_{\min}+l-1) \,] \in \mathbb{R}^{n \times ln_\xi}$$

is the propagation of cross covariance of the state $x(t)$ with $\xi(t)$,

$$T = \begin{bmatrix} G(0) & & & \\ G(1) & G(0) & & \\ \vdots & \vdots & \ddots & \\ G(i-1) & G(i-2) & \cdots & G(0) \end{bmatrix} \in \mathbb{R}^{in_y \times in_u} \tag{9}$$

is a block-lower-triangular-Toeplitz matrix of the system Markov parameters

$$G(k) = \begin{cases} 0, & k < 0, \\ D, & k = 0, \\ CA^{k-1}B, & k > 0 \end{cases}$$

$$\mathbf{R}_{u\xi} = \begin{bmatrix} \hat{R}_{u\xi}(\tau_{\min}) & \hat{R}_{u\xi}(\tau_{\min}+1) & \cdots & \hat{R}_{u\xi}(\tau_{\min}+l-1) \\ \hat{R}_{u\xi}(\tau_{\min}+1) & \hat{R}_{u\xi}(\tau_{\min}+2) & \cdots & \hat{R}_{u\xi}(\tau_{\min}+l) \\ \vdots & \vdots & & \vdots \\ \hat{R}_{u\xi}(\tau_{\min}+i-1) & \hat{R}_{u\xi}(\tau_{\min}+i) & \cdots & \hat{R}_{u\xi}(\tau_{\min}+i+l-2) \end{bmatrix} \in \mathbb{R}^{in_u \times ln_\xi}$$

is a block-Hankel matrix of the cross covariance of the input $u(t)$ and $\xi(t)$, and

$$\mathbf{R}_{v\xi} = \begin{bmatrix} \hat{R}_{v\xi}(\tau_{\min}) & \hat{R}_{v\xi}(\tau_{\min}+1) & \cdots & \hat{R}_{v\xi}(\tau_{\min}+l-1) \\ \hat{R}_{v\xi}(\tau_{\min}+1) & \hat{R}_{v\xi}(\tau_{\min}+2) & \cdots & \hat{R}_{v\xi}(\tau_{\min}+l) \\ \vdots & \vdots & & \vdots \\ \hat{R}_{v\xi}(\tau_{\min}+i-1) & \hat{R}_{v\xi}(\tau_{\min}+i) & \cdots & \hat{R}_{v\xi}(\tau_{\min}+i+l-2) \end{bmatrix} \in \mathbb{R}^{in_y \times ln_\xi}$$

is a block-Hankel matrix of the cross covariance of the noise $v(t)$ and $\xi(t)$.

Define the shifted $\mathbf{R}_{y\xi}$ as

$$\bar{\mathbf{R}}_{y\xi} = \begin{bmatrix} \hat{R}_{y\xi}(\tau_{\min}+1) & \hat{R}_{y\xi}(\tau_{\min}+2) & \cdots & \hat{R}_{y\xi}(\tau_{\min}+l) \\ \hat{R}_{y\xi}(\tau_{\min}+2) & \hat{R}_{y\xi}(\tau_{\min}+3) & \cdots & \hat{R}_{y\xi}(\tau_{\min}+l+1) \\ \vdots & \vdots & & \vdots \\ \hat{R}_{y\xi}(\tau_{\min}+i) & \hat{R}_{y\xi}(\tau_{\min}+i+1) & \cdots & \hat{R}_{y\xi}(\tau_{\min}+i+l-1) \end{bmatrix} \in \mathbb{R}^{in_y \times ln_\xi}$$

This may be expressed as

$$\bar{\mathbf{R}}_{y\xi} = \Gamma A \mathbf{R}_{x\xi} + T^+ \mathbf{R}^+_{u\xi} + \bar{\mathbf{R}}_{v\xi} \tag{10}$$

in which

$$T^+ = \begin{bmatrix} G(1) & \\ \vdots & T \\ G(i) & \end{bmatrix} \in \mathbb{R}^{in_y \times (i+1)n_u}$$

is the block-Toeplitz matrix of Markov parameters T extended by one block column and

$$\mathbf{R}^+_{u\xi} = \left[\frac{\mathbf{R}_{u\xi}}{\hat{R}_{u\xi}(\tau_{\min}+i) \cdots \hat{R}_{u\xi}(\tau_{\min}+i+l-1)} \right] \in \mathbb{R}^{(i+1)n_u \times ln_\xi}$$

is the block-Hankel matrix $\mathbf{R}_{u\xi}$ extended by one block row.

Our goal is to estimate the parameter A that appears in Eq. (10). Doing so requires isolating the row space of Γ by removing the row spaces of T and T^+ in Eqs. (7) and (10), respectively. Define the projector matrix

$$\Pi = I_{ln_\xi} - (\mathbf{R}^+_{u\xi})^T ((\mathbf{R}^+_{u\xi})(\mathbf{R}^+_{u\xi})^T)^{-1} \mathbf{R}^+_{u\xi} \in \mathbb{R}^{ln_\xi \times ln_\xi}$$

This projector has the property [7]

$$\mathbf{R}_{u\xi}\Pi = 0_{in_u \times ln_\xi} \qquad \mathbf{R}^+_{u\xi}\Pi = 0_{(i+1)n_u \times ln_\xi}$$

so that multiplication of Eqs. (7) and (10) on the right by Π results in

$$\mathbf{R}_{y\xi}\Pi = \Gamma \mathbf{R}_{x\xi}\Pi + \mathbf{R}_{v\xi}\Pi$$

and

$$\bar{\mathbf{R}}_{y\xi}\Pi = \Gamma A \mathbf{R}_{x\xi}\Pi + \bar{\mathbf{R}}_{v\xi}\Pi$$

respectively. A persistently exciting input signal is sufficient to preserve the row space of Γ in $\mathbf{R}_{y\xi}\Pi$ and $\bar{\mathbf{R}}_{y\xi}\Pi$ [15].

We are now prepared to precisely define the identification procedure. Suppose that $\hat{\Gamma}$ is an estimate of Γ. Then, the least-squares estimate of the state dynamics over one time step is

$$\hat{A} = \arg\min_{\bar{A}} \| \bar{A}\hat{\Gamma}^\dagger \mathbf{R}_{y\xi}\Pi - \hat{\Gamma}^\dagger \bar{\mathbf{R}}_{y\xi}\Pi \|_F = \Gamma^\dagger \bar{\mathbf{R}}_{y\xi}\Pi (\Gamma^\dagger \mathbf{R}_{y\xi}\Pi)^\dagger \tag{11}$$

in which $(\cdot)^\dagger$ represents the Moore–Penrose pseudoinverse. If at first the estimate $\hat{A}$ appears arbitrary, note that if Γ, $R_{y\xi}(\tau)$, and $R_{u\xi}(\tau)$ are known exactly, Eq. (11) reduces to

$$\hat{A} = \arg\min_{\bar{A}} \| (\bar{A} - A)\mathbf{R}_{x\xi}\Pi \|_F \tag{12}$$

Hence, Eq. (11) is a least-squares estimate of the propagation of $\hat{R}_{x\xi}(\tau)$ in one step of τ. Although there are several valid ways to find an estimate $\hat{\Gamma}$, we choose to employ the singular-value decomposition (SVD) of $\mathbf{R}_{y\xi}\Pi$ so that Eq. (11) reduces to a familiar closed-form expression.

To estimate Γ, first observe that $\operatorname{rank}(\Gamma) = n$, and therefore

$$\operatorname{rank}(\mathbf{R}_{y\xi}\Pi - \mathbf{R}_{v\xi}\Pi) = n$$

Thus, we choose to look for the closest rank-n matrix to $\mathbf{R}_{y\xi}\Pi$ in a 2-norm sense; that is,

$$\min_{Q}\|Q - \mathbf{R}_{y\xi}\Pi\|_2 \tag{13}$$

such that $\text{rank}(Q) = n$.

Define the SVD

$$\mathbf{R}_{y\xi}\Pi = [\,U_n \quad U_s\,]\begin{bmatrix}\Sigma_n & 0\\ 0 & \Sigma_s\end{bmatrix}\begin{bmatrix}V_n^T\\ V_s^T\end{bmatrix} \tag{14}$$

in which Σ_n is a diagonal matrix containing the first n singular values of $\mathbf{R}_{y\xi}\Pi$, and Σ_s contains the remaining $s = in_y - n$ singular values. The solution to Eq. (13) is then [16]

$$Q = U_n\Sigma_n V_n^T$$

Moreover, the error is given by

$$\sigma_{n+1} = \|U_n\Sigma_n V_n^T - \mathbf{R}_{y\xi}\Pi\|_2$$

so that if the system order n is unknown, it may be estimated by examining the singular values of $\mathbf{R}_{y\xi}\Pi$ and searching for a significant dropoff.

We then let Q be an estimate of $\mathbf{R}_{y\xi}\Pi$. $\hat{\Gamma}$ may then be taken from any valid-dimensioned factorization of Q. We choose the factorization

$$\hat{\Gamma} = U_n\Sigma^{1/2} \qquad \mathbf{R}_{x\xi}\Pi = \Sigma^{1/2}V_n^T \tag{15}$$

With $\hat{\Gamma}$ taken from Eq. (15), Eq. (11) reduces to

$$\hat{A} = \hat{\Gamma}^{\dagger}\bar{\mathbf{R}}_{y\xi}\Pi(\hat{\Gamma}\mathbf{R}_{y\xi}\Pi)^{\dagger} = \Sigma_n^{-1/2}U_n^T\bar{\mathbf{R}}_{y\xi}\Pi V_n\Sigma_n^{-1/2} \tag{16}$$

With $\hat{C}$ an estimate of C taken from the first n_y rows of $\hat{\Gamma}$, B and D can be shown to be linear in the relationship between $R_{y\xi}(\tau)$ and $R_{u\xi}(\tau)$, and thus solvable via a linear least-squares problem ([13], page 342; and [17]).

Many modifications to traditional subspace identification methods can be applied to the described algorithm with similar benefits, such as implementation of the projection by means of the decomposition of a matrix into an orthogonal matrix and upper-triangular matrix ([6], pages 155–156) and replacing the orthogonal projection with an oblique projection ([18], page 21).

III. Identification of Aeroservoelastic Dynamics

The COBRA method was applied to in-flight data taken from accelerometer and pressure measurements onboard an F/A-18 located at NASA's Dryden Flight Research Center that has been modified for aeroelastic research. The algorithm requires careful selection of the instrument signal $\xi(t)$ to ensure that the system estimate is unbiased. If $\xi(t)$ is chosen incorrectly, the result may be biased by either the noise process or unwanted system dynamics. In the following two examples, the choice of an appropriate $\xi(t)$ is discussed in detail.

A. Collective Leading-Edge Flap Excitation

Consider the identification of the response from the leading-edge flap (LEF) to the acceleration and pressure sensors. Signal pathways for the system are shown in Fig. 1, in which G_{lef} is the collective LEF actuator dynamics and G the ASE dynamics of interest. The collective LEF position $u(t)$ is perturbed by a noise signal $v_{\text{lef}}(t)$ that must be assumed correlated with the noise $v(t)$ on the acceleration

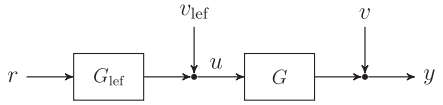

Fig. 1 Leading-edge flap experiment signal pathways.

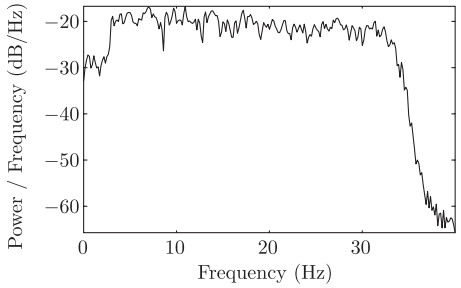

Fig. 2 PSD of OBES signal for collective LEF excitation.

and pressure measurements $y(t)$. The result is that identification directly from $u(t)$ to $y(t)$ will be biased by the cross spectrum of the two noise signals, regardless of the identification algorithm used, unless steps are taken to decorrelate them from the noise.

The reference excitation $r(t)$ was chosen to be a minimax crest factor multisine [19] of bandwidth between 3 and 35 Hz. The power-spectral density (PSD) of $r(t)$ is shown in Fig. 2. It can be seen that $r(t)$ closely resembles white noise in the frequency range of interest. The signal $r(t)$ is uncorrelated with either noise signal, since it is deterministic; it may also be treated as quasi stationary, since as a sum of sinusoids, its autocovariance function exists. Hence, the mapping between the cross-covariance functions $R_{yr}(\tau)$ and $R_{ur}(\tau)$ is limited

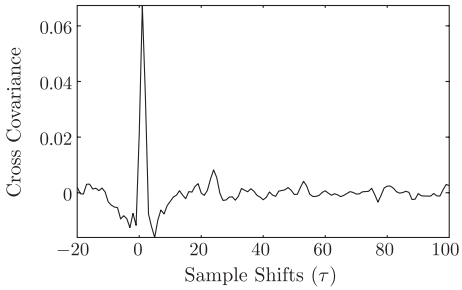

Fig. 3 Cross-covariance-function estimate between collective LEF position (u) and reference (r) for LEF excitation.

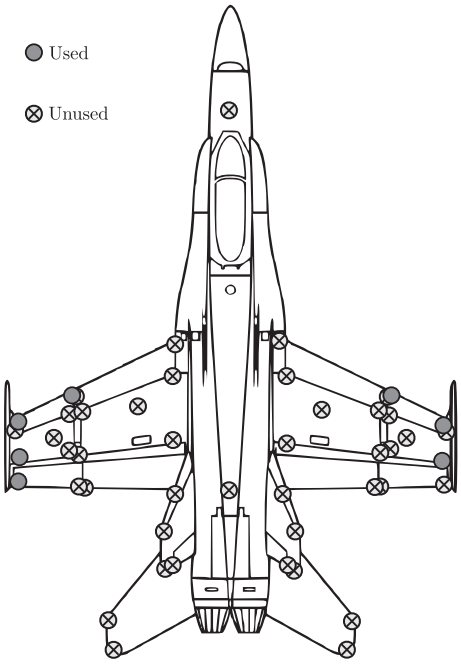

Fig. 4 Locations of used and unused accelerometers for the collective LEF experiment.

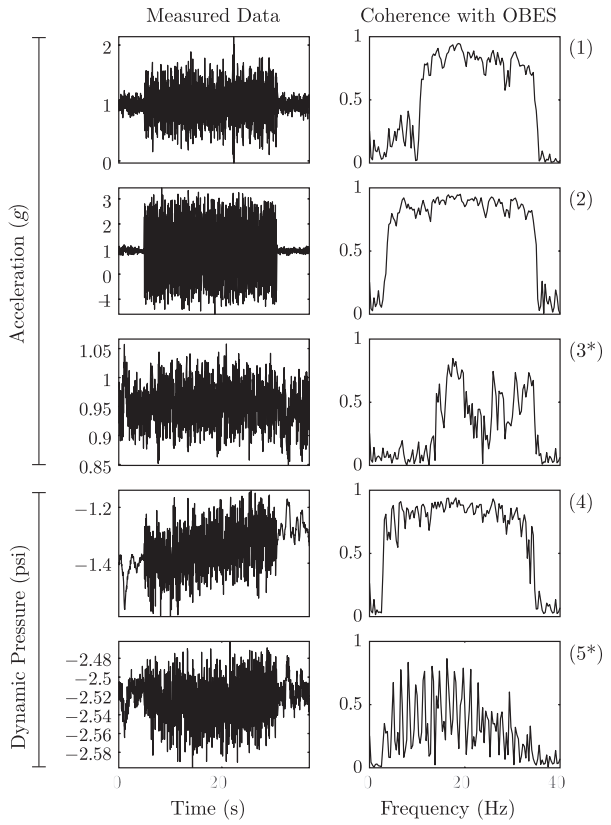

Fig. 5 Sample of signals measured for the collective leading-edge flap experiment. Signals with ∗ did not meet coherence threshold and were not used for identification.

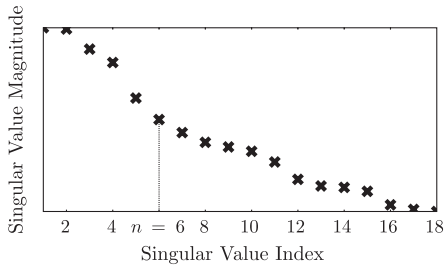

Fig. 6 Singular values of the projected data matrix for the collective LEF experiment (*y* axis in log scale).

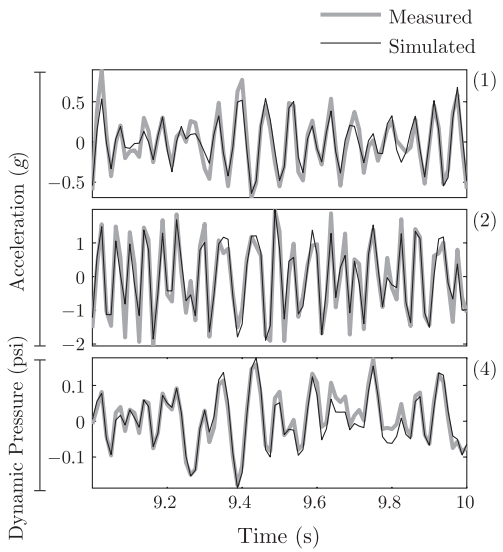

Fig. 7 Sample of simulation results of the collective LEF experiment.

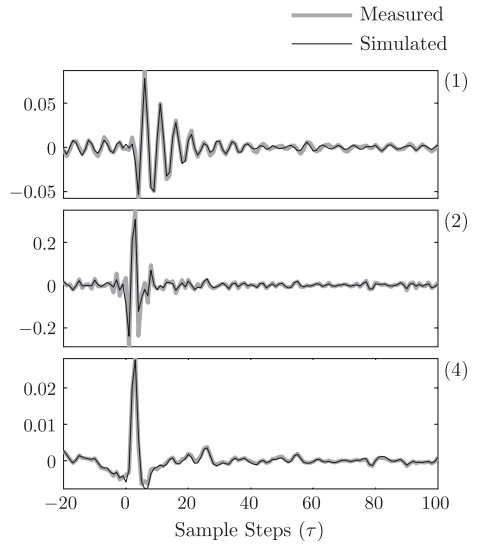

Fig. 8 Sample of simulation cross-covariance estimates of the collective LEF experiment.

to the dynamics G, and we select $\xi(t) = r(t)$ when analyzing the data.

The cross-covariance estimate $\hat{R}_{ur}(\tau)$ is shown in Fig. 3. Only the data in which the excitation signal $r(t)$ is nonzero were used to calculate the PSD and cross-covariance functions. The cross-covariance functions were further truncated to $\tau \in [-20, 100]$ after calculation for identification purposes, since as τ increases, the signal-to-noise ratio of the cross-covariance estimates becomes prohibitively small.

Because 94 signals were available for use, an objective criteria was created to determine which had a sufficiently high signal-to-noise ratio. Only signals that had magnitude-square coherence with $r(t)$ of at least $\frac{2}{3}$ averaged over the frequency range 3–35 Hz were selected from the available measurements. The locations of used and unused accelerometers are shown in Fig. 4. Only the top-front-left pressure sensor was used. Although only eight total signals were used for

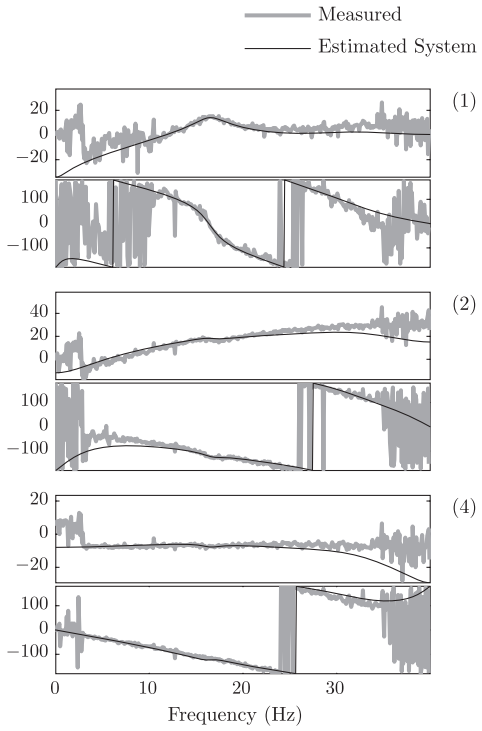

Fig. 9 Bode plot of the estimated system and spectral estimate of the collective LEF experiment. Magnitude is in dB, and phase is in degrees.

identification in this experiment, the collective LEF input is intended to excite neither rigid-body moments nor bending moments on the wing, so the low number of usable signals is expected. Excitation of other surfaces will naturally produce different selections of signals. A sample of signals is shown in Fig. 5.

A model was constructed using the COBRA method proposed in Sec. II. The singular values of the matrix [Eq. (14)] are shown in Fig. 6. The system order was chosen to be $n = 6$, which is just before the magnitude of the singular values appears to flatten out.

Time-domain simulations of the estimated model are shown with the data in Fig. 7. Cross-covariance estimates from the simulated data and measured data are shown in Fig. 8. Finally, Bode plots of the estimated system are compared with spectral estimates [computed from the cross spectrum of $y(t)$ with $r(t)$ and $u(t)$ with $r(t)$] in Fig. 9.

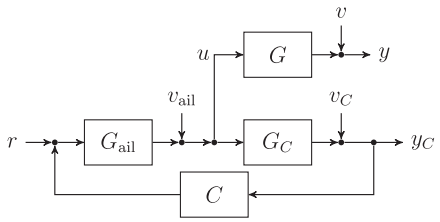

Fig. 10 Aileron experiment signal pathways.

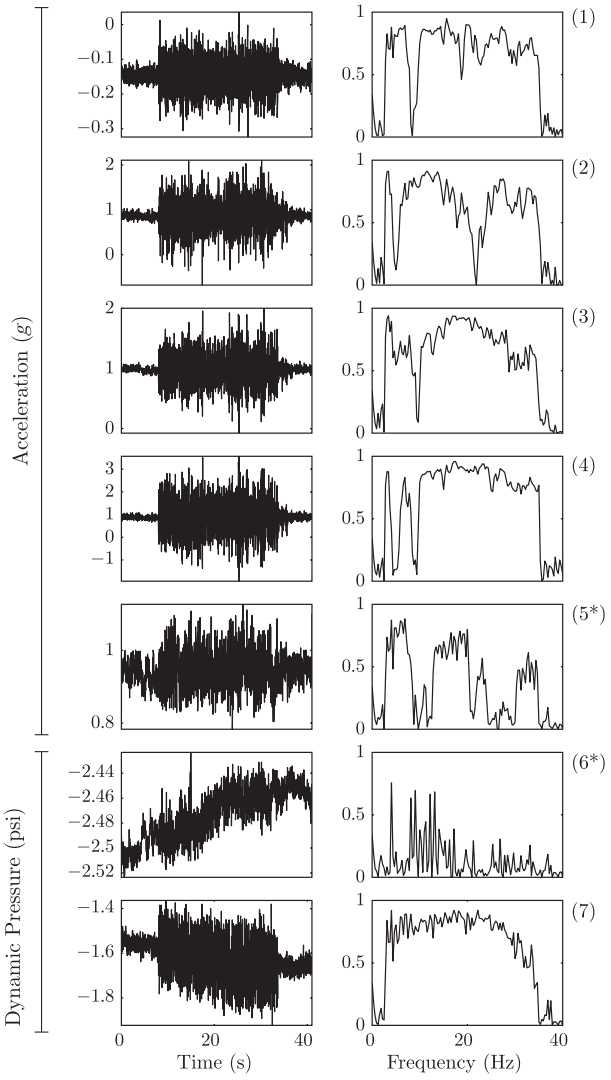

Fig. 11 Sample of signals used for the differential aileron experiment.

B. Differential Aileron Excitation

Next, consider the identification from the differential aileron input to the acceleration and pressure sensors. Signal pathways are shown in Fig. 10. As before, the input $u(t)$ is perturbed by a noise signal $v_{\text{ail}}(t)$ and the output $y(t)$ by a noise signal $v(t)$. Additionally, the system contains a feedback controller C, which augments the excitation $r(t)$ with a differential aileron command. The feedback signals to the control system $y_C(t)$ are the result of both rigid-body and ASE dynamics, represented in a combined system G_C. The feedback $y_C(t)$ also contains a noise signal $v_C(t)$, which must be assumed correlated with $v_{\text{ail}}(t)$ and $v(t)$.

Because $v_C(t)$ appears in $u(t)$ after being filtered through the dynamics of G_C, C, and the aileron servo G_{ail}, direct identification using $u(t)$ to $y(t)$ will provide an estimate biased by the subsystems G_{ail}, G_C, and C in addition to the various cross spectra of $v(t)$, $v_{\text{ail}}(t)$, and $v_C(t)$. As before, however, the reference $r(t)$ is uncorrelated with the noise signals and may be used as an instrument $\xi(t) = r(t)$ to provide unbiased results.

Sample signals are shown in Fig. 11. The same coherence-based criteria of the LEF experiment was used to determine which signals were acceptable for identification purposes; signals marked by $*$ were designated unacceptable and not used. A total of 49 output signals were used for identification purposes for this experiment.

Locations of all used and unused accelerometers are shown in Fig. 12. Observe that the usable accelerometers are distributed

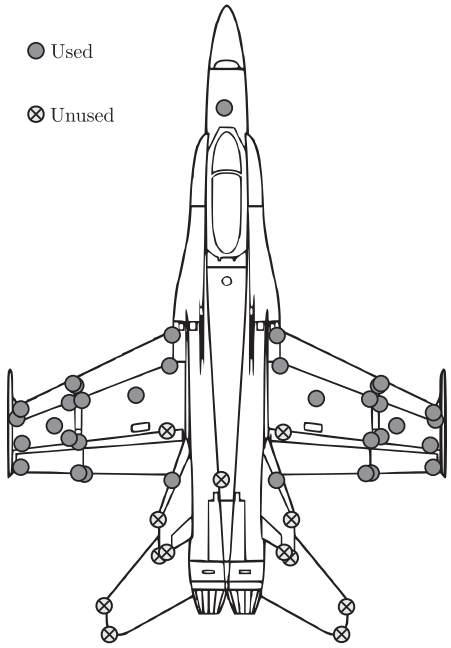

Fig. 12 Locations of used and unused accelerometers for the differential aileron experiment.

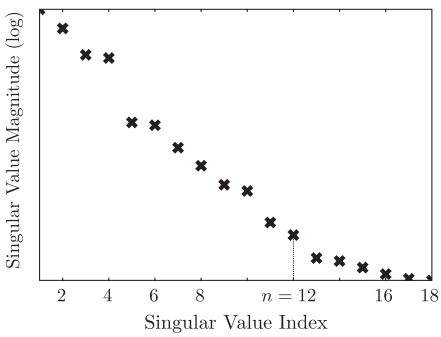

Fig. 13 Singular values of the projected data matrix for the differential aileron experiment.

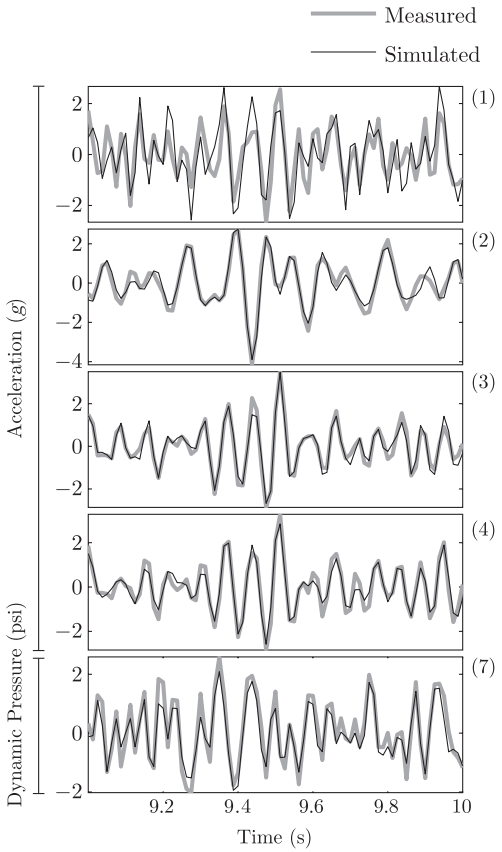

Fig. 14 Sample of simulation results of the differential aileron experiment.

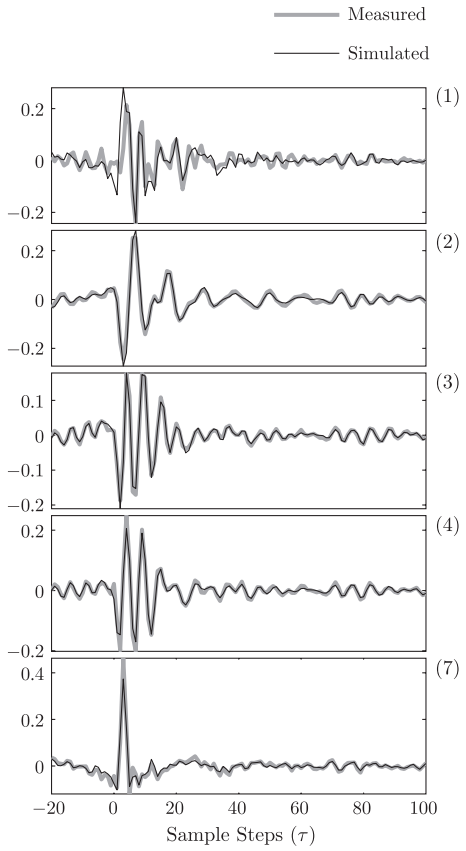

Fig. 15 Sample of simulation cross-covariance estimates of the differential aileron experiment.

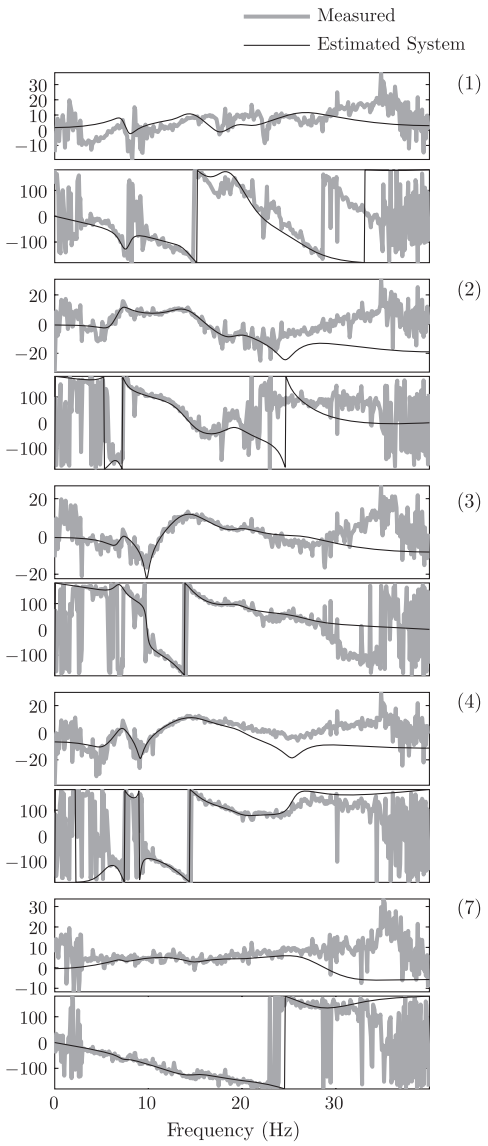

Fig. 16 Bode plot of the estimated system and spectral estimate of the differential aileron experiment. Magnitude is in dB, and phase is in degrees.

primarily over the wings, as one would expect from a differential aileron excitation. The selected accelerometer in the nose measures lateral motion, explaining its high coherence with $r(t)$.

A model was again constructed using the method proposed in Sec. II. The singular values of the projected data matrix [Eq. (14)] are shown in Fig. 13. The system order was chosen to be $n = 12$, which is naturally larger than that of the LEF experiment due to the increase in the output dimension n_y. Additionally, the ailerons have much more inertial excitation than the LEFs, being heavier and a larger geometric proportion of the wings, so more response is expected overall.

Samples of five estimated signal pathways for the 49 used output signals are shown in Figs. 14–16. Time-domain simulations are plotted with measured data in Fig. 14, and comparisons with cross-covariance-function estimates are plotted in Fig. 15. The enumeration is the same as in Fig. 11. Spectral estimates and Bode plots of the estimated system are shown in Fig. 16.

IV. Conclusions

A novel subspace identification algorithm has been presented that produces accurate, unbiased, linear models from measured data of a large signal dimension (i.e., data acquired from many sensors). The algorithm employs covariance-function estimates, uses a

dynamic-invariance property of the output signals with a strong relationship to classical realization theory, relies exclusively on reliable numerical linear algebra techniques, and requires no iterative solution. The convergence of covariance-function estimates is used to handle large data sets in both open- and closed-loop experiments. The algorithm has been successfully applied to data measured in flight from the NASA Active Aeroelastic Wing F/A-18 for both open-loop and closed-loop experiments.

As a final note, it is mentioned that the algorithm is capable of analyzing data from multiple inputs and references and would, in theory, provide similar results were the two experiments combined into a single experiment. Data for such an experiment, however, are currently unavailable to the authors.

Appendix

This appendix discusses the relationship of the COBRA method to similar subspace identification methods. It is shown that, when a purely white-noise input is used and the covariance-function estimates computed over a specific domain, the algorithm asymptotically generalizes to the well-known eigensystem realization algorithm.

I. Relationship to the Eigensystem Realization Algorithm

When the input data are purely white, the preceding algorithm can be shown to reduce to a realization algorithm from noise-corrupted Markov parameters due to the autocovariance function of the input approaching a unit impulse [24].

To see this, let H be a block-Hankel matrix of system Markov parameters starting at $G(1)$,

$$H = \begin{bmatrix} G(1) & G(2) & G(3) & \cdots \\ G(2) & G(3) & G(4) & \cdots \\ \vdots & \vdots & \vdots & \\ G(i) & G(i+1) & G(i+2) & \cdots \end{bmatrix} \in \mathbb{R}^{in_y \times \infty}$$

and let $\bar{H}$ be a block-Hankel matrix of Markov parameters starting at $G(2)$,

$$\bar{H} = \begin{bmatrix} G(2) & G(3) & G(4) & \cdots \\ G(3) & G(4) & G(5) & \cdots \\ \vdots & \vdots & \vdots & \\ G(i+1) & G(i+2) & G(i+3) & \cdots \end{bmatrix} \in \mathbb{R}^{in_y \times \infty}$$

Data-matrix equations (7) and (10) can be expressed as

$$\mathbf{R}_{y\xi} = H\mathbf{R}^{p}_{u\xi} + T\mathbf{R}_{u\xi} + \mathbf{R}_{v\xi}$$

and

$$\bar{\mathbf{R}}_{y\xi} = \bar{H}\mathbf{R}^{p}_{u\xi} + T^{+}\mathbf{R}^{+}_{u\xi} + \bar{\mathbf{R}}_{v\xi}$$

respectively, where $\mathbf{R}^{p}_{u\xi}$ is a block-Toeplitz matrix of input data,

$$\mathbf{R}^{p}_{u\xi} = \begin{bmatrix} \hat{R}_{u\xi}(\tau_{\min}-1) & \hat{R}_{u\xi}(\tau_{\min}) & \cdots & \hat{R}_{u\xi}(\tau_{\min}+l-2) \\ \hat{R}_{u\xi}(\tau_{\min}-2) & \hat{R}_{u\xi}(\tau_{\min}-1) & \cdots & \hat{R}_{u\xi}(\tau_{\min}+l-3) \\ \hat{R}_{u\xi}(\tau_{\min}-3) & \hat{R}_{u\xi}(\tau_{\min}-2) & \cdots & \hat{R}_{u\xi}(\tau_{\min}+l-4) \\ \vdots & \vdots & & \vdots \end{bmatrix} \in \mathbb{R}^{\infty \times l}$$

Suppose $u(t)$ is a noise-free white-noise input, and let $\xi(t) = u(t-1)$. Then, $\hat{R}_{u\xi}(\tau)$ will converge to a unit pulse at $\tau = -1$ as $N \to \infty$. Let $\tau_{\min} = 0$ and $i > n$. Then, $\mathbf{R}_{y\xi} = 0$, $\Pi = I_l$, and $H\mathbf{R}^{p}_{u\xi}$ and $\bar{H}\mathbf{R}^{p}_{u\xi}$ become finite products where the first l rows of $\mathbf{R}^{p}_{u\xi}$ are I_l and the rest are 0. Hence, as the number of samples used to construct the cross-covariance-function estimates $N \to \infty$,

$$\mathbf{R}_{y\xi} \to H \qquad \bar{\mathbf{R}}_{y\xi} \to \bar{H}$$

Thus, Eq. (16) will asymptotically become a construction of a state-space realization from estimates of Markov parameters by means of the SVD, which is the main step of the ERA [10].

II. Relationship to Other Subspace Identification Methods

The algorithm proposed in this paper differs from classical subspace algorithms in two critically significant ways: we propose to solve for the system dynamics based on variation of covariance-function estimates, and we solve for the system matrices, based not on the shift invariance of the extended observability matrix but on the one-time-step variation of the measured data.

When the instrument $\xi(t)$ is chosen to be the input signal $u(t)$ or the composite signal $\xi(t) = [\, y^T(t) \quad u^T(t)\,]^T$, the algorithm resembles the MOESP family of algorithms [20], which can be shown to reduce to forming cross-covariance estimates between the output and input during the projection step [21]. However, because PI-MOESP, PO-MOESP, and their related variants, such as robust N4SID ([18], page 112; and [22]), rely on the null-space projection to decorrelate the noise from the output data, they will only produce unbiased estimates when the input is noise free [23]. Additionally, the orthogonal projection must be replaced with an oblique projection to guarantee unbiased estimates in the case of colored output noise [20], which effectively limits the size of the data matrices available for identification since some rows of the data matrices must be selected to construct an oblique subspace.

An extension of MOESP has been proposed in which the system is perturbed by input, output, and state noise, which may all be correlated, so long as all noise signals are white, and this approach may be extended to the closed-loop case [23]. If the input or output measurement noise is colored, however, the estimates will once again become biased. Moreover, few of the methods address the issue of bias on the estimates of B and D, which determine the location of the system zeros. Identification via covariance-function estimates inherently guarantees that the identification will be constrained to the deterministic content of the data for all linear time-invariant systems. Additionally, because covariance-function estimates may be computed via the fast Fourier transform, effectively pre-averaging the data, the amount of data that can be used for estimation purposes dramatically increases.

References

[1] Brenner, M. J., Lind, R. C., and Voracek, D. F., "Overview of Recent Flight Flutter Testing Research at NASA Dryden," NASA Dryden Flight Research Center NASA-TM-4792, Edwards, CA, 1997.

[2] Van Overschee, P., and De Moor, B., "A Unifying Theorem for Three Subspace System Identification Algorithms," *Automatica*, Vol. 31, No. 12, Dec. 1995, pp. 1853–1864. doi:10.1016/0005-1098(95)00072-0

[3] Mehra, R., Mahmood, S., and Waissman, R., "Identification of Aircraft and Rotorcraft Aeroelastic Modes Using State Space System Identification," *Proceedings of the 4th IEEE Conference on Control Applications*, IEEE, Piscataway, NJ, 1995, pp. 432–437. doi:10.1109/CCA.1995.555742

[4] Mevel, L., Goursat, M., Benveniste, A., and Basseville, M., "Aircraft Flutter Test Design Using Identification and Simulation: a SCILAB Toolbox," *Proceedings of 2005 IEEE Conference on Control Applications*, Toronto, IEEE, Piscataway, NJ, 2005, pp. 1115–1120. doi:10.1109/CCA.2005.1507280

[5] Mevel, L., Benveniste, A., Basseville, M., Goursat, M., Peeters, B., Van der Auweraer, H., and Vecchio, A., "Input/Output Versus Output-Only Data Processing for Structural Identification: Application to In-Flight Data Analysis," *Journal of Sound and Vibration*, Vol. 295, Nos. 3–5, Aug. 2006, pp. 531–552. doi:10.1016/j.jsv.2006.01.039

[6] Katayama, T., "Subspace Methods for System Identification," *Communications and Control Engineering*, Springer–Verlag, London, 2005, pp. 155–156, 253–254.

[7] Miller, D. N., and de Callafon, R. A., "Subspace Identification Using Dynamic Invariance in Shifted Time-Domain Data," *49th IEEE Conference on Decision and Control (CDC)*, Atlanta, GA, IEEE, Piscataway, NJ, Dec. 2010, pp. 2035–2040.

doi:10.1109/CDC.2010.5717151

[8] Verboven, P., Cauberghe, B., Guillaume, P., Vanlanduit, S., and Parloo, E., "Modal Parameter Estimation and Monitoring for On-Line Flight Flutter Analysis," *Mechanical Systems and Signal Processing*, Vol. 18, No. 3, 2004, p. 24.
doi:10.1016/S0888-3270(03)00074-8

[9] Baldelli, D. H., Zeng, J., Lind, R. C., and Harris, C., "Flutter-Prediction Tool for Flight-Test-Based Aeroelastic Parameter-Varying Models," *Journal of Guidance, Control, and Dynamics*, Vol. 32, No. 1, Jan. 2009, pp. 158–171.
doi:10.2514/1.36584

[10] Juang, J.-N., and Pappa, R. S., "An Eigensystem Realization Algorithm (ERA) for Modal Parameter Identification and Model Reduction," *JPL Proceedings of the Workshop on Identification and Control of Flexible Space Structures*, Vol. 3, NASA, April 1985, pp. 299–318.

[11] Juang, J.-N., Phan, M. Q., Horta, L. G., and Longman, R. W., "Identification of Observer/Kalman Filter Markov Parameters: Theory and Experiments," *Journal of Guidance, Control, and Dynamics*, Vol. 16, No. 2, 1993, pp. 320–329.
doi:10.2514/3.21006

[12] Chiuso, A., "The Role of Vector Autoregressive Modeling in Predictor-Based Subspace Identification," *Automatica*, Vol. 43, No. 6, June 2007, pp. 1034–1048.
doi:10.1016/j.automatica.2006.12.009

[13] Ljung, L., "System Identification: Theory for the User," *PTR Prentice Hall Information and System Sciences*, 2nd ed., Prentice–Hall PTR, Upper Saddle River, NJ, 1999, pp. 32, 342, 434.

[14] Chen, C.-T., *Linear System Theory and Design*, 1st ed., Oxford Univ. Press, New York, 1984, p. 233.

[15] Willems, J., Rapisarda, P., Markovsky, I., and De Moor, B., "A Note on Persistency of Excitation," *Systems and Control Letters*, Vol. 54, No. 4, April 2005, pp. 325–329.
doi:10.1016/j.sysconle.2004.09.003

[16] Golub, G., and Van Loan, C., *Matrix Computations*, 3rd ed., Johns Hopkins Univ. Press, Baltimore, MD, 1996, p. 72.

[17] Miller, D. N., and de Callafon, R. A., "Ecient Identification of Input Dynamics for Correlation Function-Based Subspace Identification," *Proceedings of the 18th IFAC World Congress*, Elsevier, Milan, 2011, pp. 6511–6516.
doi:10.3182/20110828-6-IT-1002.02597

[18] Van Overschee, P., and De Moor, B., *Subspace Identification for Linear Systems: Theory, Implementation, Applications*, Kluwer Academic, London, 1996, pp. 21, 112.

[19] Pintelon, R., and Schoukens, J., *System Identification: A Frequency Domain Approach*, Wiley-IEEE Press, New York, Jan. 2001, pp. 129–130.

[20] Verhaegen, M., and Verdult, V., *Filtering and System Identification: A Least Squares Approach*, 1st ed., Cambridge Univ. Press, New York, May 2007, pp. 327–329.

[21] Viberg, M., Wahlberg, B., and Ottersten, B., "Analysis of State Space System Identification Methods Based on Instrumental Variables and Subspace Fitting," *Automatica*, Vol. 33, No. 9, Sept. 1997, pp. 1603–1616.
doi:10.1016/S0005-1098(97)00097-6

[22] "MATLAB System Identification Toolbox," The Mathworks, Natick, MA, 2009.

[23] Chou, C., and Verhaegen, M., "Subspace Algorithms for the Identification of Multivariable Dynamic Errors-in-Variables Models," *Automatica*, Vol. 33, No. 10, Oct. 1997, pp. 1857–1869.
doi:10.1016/S0005-1098(97)00092-7

[24] Kung, S.-Y., "A New Identification and Model Reduction Algorithm via Singular Value Decomposition," *Proceedings of the 12th Asilomar Conference on Circuits, Systems, and Computers*, IEEE, Piscataway, NJ, 1978, pp. 705–714.